Electrochemistry and Electrogenerated Chemiluminescence of (dppy)BTPA—a Bipolar, Solvatochromic Boron Compound

Matthew M. Sartin,[†] Hongyu Zhang,[‡] Jingying Zhang,[‡] Peng Zhang,[‡] Wenjing Tian,[‡] Yue Wang,[‡] and Allen J. Bard*[,†]

The University of Texas at Austin, Chemistry and Biochemistry Department, Austin, Texas 78712, and Key Laboratory for Supramolecular Structure and Materials of Ministry of Education, College of Chemistry, Jilin University, Changchun, 130012, P. R. China

Received: May 29, 2007; In Final Form: July 26, 2007

We investigated the electrochemistry and electrogenerated chemiluminescence (ECL) of the highly solvatochromic emitter (dppy)BTPA, which consists of a 2,6-diphenolpyridine (dppy) boron moiety linked to a triphenylamine moiety (BTPA). At 0.72 V versus a saturated calomel electrode (SCE), in pure MeCN, the triphenylamine moiety of (dppy)BTPA is oxidized to form a stable radical cation. At −1.72 V versus SCE, in pure MeCN, the diphenolpyridine boron moiety is reduced to form a radical anion that dimerizes with $k_f = 1.8 \times 10^4$ M^{-1} s^{-1}. Annihilation between the two radical ions generates an ECL spectrum in the same region as the photoluminescence (PL) spectrum, but with an additional shoulder at a longer wavelength. Both the PL and the ECL exhibit a strong bathochromic shift and quenching as solvent polarizability increases (for different solvents or for mixtures of MeCN and benzene). This effect is enhanced by the presence of the supporting electrolyte, $Bu_4N^+ClO_4^-$.

Introduction

The bipolar molecule (dppy)BTPA (Figure 1) consists of a 2,6-diphenolpyridine boron moiety[1] and a triphenylamine moiety. Molecular orbital calculations show that the dppy and Ph_3N act as electron donor and acceptor centers, respectively.[2] Their spatial separation lends strong charge transfer (CT) character to the excited-state of (dppy)BTPA, resulting in highly solvatochromic emissions. This property, combined with the high electron and hole mobility of solid (dppy)BTPA, has been exploited to make an efficient, single-layer electroluminescent device.[3] These properties also make (dppy)BTPA an interesting candidate for electrogenerated chemiluminescence (ECL) studies.

The ECL of organic molecules is typically brought about by a reaction between a radical anion and cation to generate an emissive excited species.[4] The energy available for excited-state generation is approximately equal to the enthalpy of annihilation: $-\Delta H^\circ = -\Delta G^\circ - T\Delta S^\circ$ ($T\Delta S^\circ \approx 0.1$ V). If $-\Delta H^\circ$ is greater than the energy of an excited state, E_S (singlet) or E_T (triplet), a molecule can achieve that state upon radical ion annihilation. If the singlet state is directly populated, then the ECL mechanism is referred to as S-route ECL. If the triplet state is populated, triplet−triplet annihilation can occur to create a singlet state in what is known as T-route ECL. The radical ions are usually generated at a single electrode by alternately pulsing between oxidizing and reducing potentials. However, instability of either radical ion results in a rapid loss of ECL intensity with successive pulses. Using shorter pulse widths can overcome this problem by creating the other radical ion before the unstable one can decompose, but the RC time constant for charging the electrode surface limits the minimum pulse width. The use of small electrodes to reduce the time constant also lowers the overall light intensity.

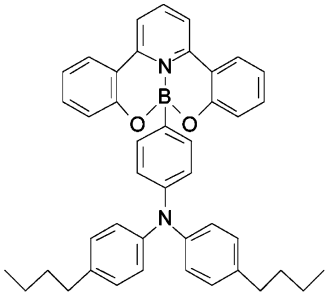

Figure 1. Structure of (dppy)BTPA.

If one radical ion is too unstable, ECL can also be generated with a coreactant, such as benzoyl peroxide (BPO), which forms a strong oxidizing agent ($E^\circ = +0.8$ V[5] or $+1.5$ V[6]) after being reduced.[7] This can react directly with the analyte anion and generate light without the radical cation. The general mechanism, using BPO, is given by the following reactions.

$$BPO + e^- \rightarrow BPO^{\bullet -} \quad (1)$$

$$BPO^{\bullet -} \rightarrow C_6H_5CO_2^- + C_6H_5CO_2^{\bullet} \quad (2)$$

$$C_6H_5CO_2^{\bullet} + R^{\bullet -} \rightarrow C_6H_5CO_2^- + R^* \quad (3)$$

Solvatochromism is not often examined in ECL. Previous ECL studies of CT emitters have focused on quantum efficiencies and electron-transfer rates of a variety of molecules,[8] as well as the effects of solvent[9] and electrolyte.[10] However, these studies do not explore the solvatochromic shift of the ECL. The photoluminescence (PL) of (dppy)BTPA exhibits a linear bathochromic shift with respect to increasing solvent polariz-

* Corresponding author. E-mail: ajbard@mail.utexas.edu.
[†] The University of Texas at Austin.
[‡] Key Laboratory of Supramolecular Structure and Materials of Ministry of Education.

10.1021/jp0741509 CCC: $37.00 © 2007 American Chemical Society
Published on Web 10/04/2007

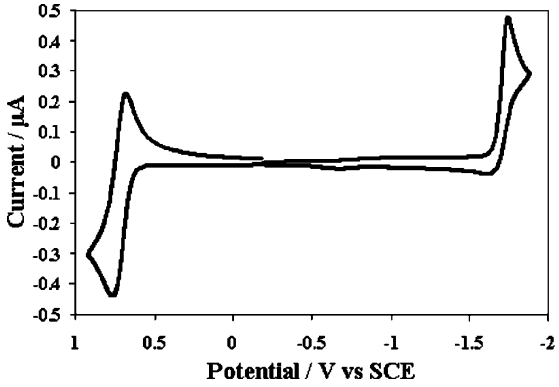

Figure 2. Cyclic voltammogram of 1 mM (dppy)BTPA in acetonitrile with 0.1 M TBAP at $\upsilon = 50$ mV/s; $E^{\circ}_{ox} = 0.72$ V vs SCE, $E^{\circ}_{red} = -1.72$ V vs SCE, and $k^{\circ} = 1.8 \times 10^4$ $M^{-1}s^{-1}$.

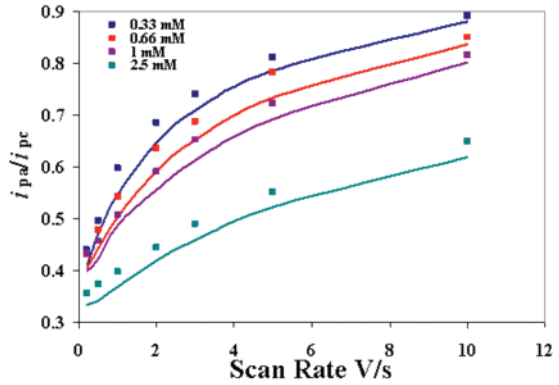

Figure 3. Experimental (squares) and simulated (lines) scan rate dependence of the peak current ratio of the (dppy)BTPA reduction wave at various concentrations.

ability,[11] which permits comparison between efficiencies and emission wavelengths for the ECL and (dppy)BTPA.

In this paper, we investigate the ECL of (dppy)BTPA and compare the solvatochromic shift and quantum efficiency trends to those of the PL. In the process, we employ cyclic voltammetry to examine the stability of the radical ions and the mechanism of their decomposition.

Experimental

Materials. Anhydrous MeCN was obtained from Aldrich (St. Louis, MO) and transferred into a helium atmosphere drybox (Vacuum Atmospheres Corp., Hawthorne, CA) without further purification. Anhydrous benzene was obtained from Aldrich and distilled under vacuum to remove an electroactive impurity before being transferred to the drybox. All other solvents were obtained from Fisher (Fair Lawn, NJ) or Aldrich and used as received. Electrochemical grade tetra-*n*-butylammonium perchlorate (TBAP) was obtained from Fluka and transferred directly into the drybox. The (dppy)BTPA compound was synthesized according to literature procedures.[3] Benzoyl peroxide (BPO) was obtained from Aldrich and was used as received.

Characterization. The electrochemical cell for cyclic voltammetry (CV) and ECL transients consisted of a 1.5 mm Pt disk inlaid in glass as the working electrode (WE), a coiled Pt wire as the counter electrode (CE), and a Ag wire quasireference electrode (QRE). The potential of the QRE was calibrated using ferrocene (0.342 V vs a saturated calomel electrode (SCE)) as an internal standard.[12] Before each experiment, the WE was polished with 0.3 μm alumina (Buehler, Ltd., Lake Bluff, IL), sonicated in water, and then sonicated in ethanol, for 1 min each. The electrode was then rinsed with acetone before being transferred into the dry box. For ECL spectra, the WE was a 1.5 mm Pt disk inlaid in glass and bent at a 90° angle so that the electrode surface faced the detector. A 25 μm ultramicroelectrode (UME), polished using 0.05 μm alumina, was used for steady-state and fast scan experiments.

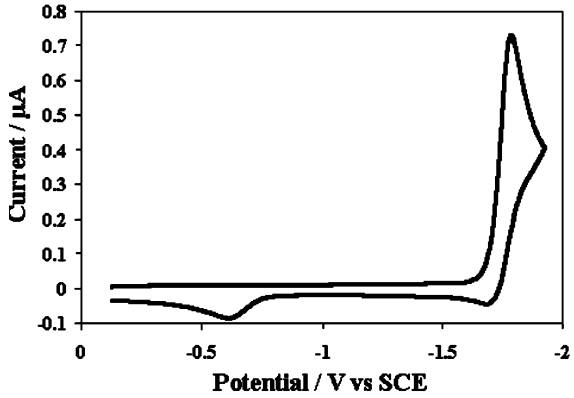

Figure 4. Reduction of 1 mM (dppy)BTPA in MeCN with 0.1 M TBAP. Second reverse wave appears at −0.59 V vs SCE.

All solutions for electrochemical measurements consisted of 0.1 M TBAP as the supporting electrolyte and 1 mM (dppy)-BTPA (except where otherwise noted) in various ratios of benzene to MeCN. Solutions were prepared inside the dry box. For measurements made outside of the box, the electrochemical cell was closed with a Teflon cap sealed with a rubber O-ring. Stainless steel rods driven through the cap formed the electrode connections. Cyclic voltammograms were performed using a CH Instruments model 660 Electrochemical Workstation (Austin, TX).

Digital simulations of cyclic voltammograms were performed using the DigiElch software package[13] and DigiSim (Bioanalytical Systems). The uncompensated resistance and capacitance were determined from the current−time curve for a potential step in a nonfaradaic potential region of the background solution. The diffusion coefficient of (dppy)BTPA ($D = 5.8 \times 10^{-6}$ cm^2/s) was obtained by averaging the D value obtained from a potential step experiment with that obtained from the peak currents of CVs performed at scan rates from 50 mV/s to 10 V/s. For simulations, all products of the electrochemical processes were assigned the same diffusion coefficient as (dppy)BTPA. The electrode surface area was determined from a Cottrell plot of a potential step experiment in 1 mM ferrocene in MeCN ($D = 1.2 \times 10^{-5}$ cm^2/s).[14]

For spectroscopy, (dppy)BTPA solutions were prepared in a 1 cm quartz cell. Absorbance spectra were collected on a DU 640 spectrophotometer (Beckman, Fullerton, CA). Fluorescence spectra were collected on a QuantaMaster spectrofluorimeter (Photon Technology International, Birmingham, NJ). The excitation source was a 70W xenon lamp, and the slits for excitation and emission were 0.2 mm for all samples, except those in MeCN and DMSO, which used 1 mm. Quantum efficiencies were determined with respect to $Ru(bpy)_3^{2+}$ ($\Phi_{PL} = 0.075$).[15]

To generate ECL, the working electrode was pulsed at 5 Hz between potentials 80 mV beyond the diffusion-limited peak potentials (E_p) corresponding to the reduction and oxidation of (dppy)BTPA. Coreactant ECL experiments were performed with 1 mM (dppy)BTPA, 10 mM BPO, and 0.1 M TBAP in MeCN, and the pulses were between 0 V and $E_{p,red} - 0.08$ V. The potential pulses were generated by an Eco Chemie Autolab potentiostat (The Netherlands). Spectra were collected on a

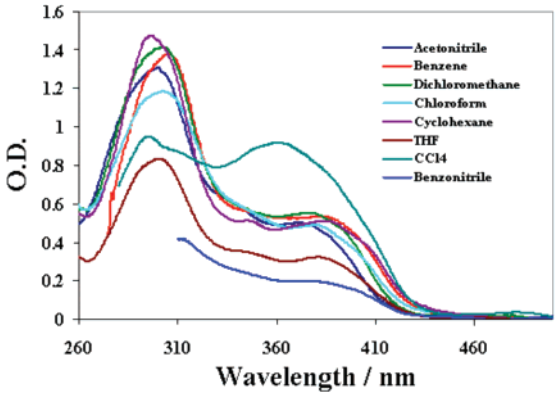

Figure 5. Absorbance spectra of 50 μM (dppy)BTPA in various solvents.

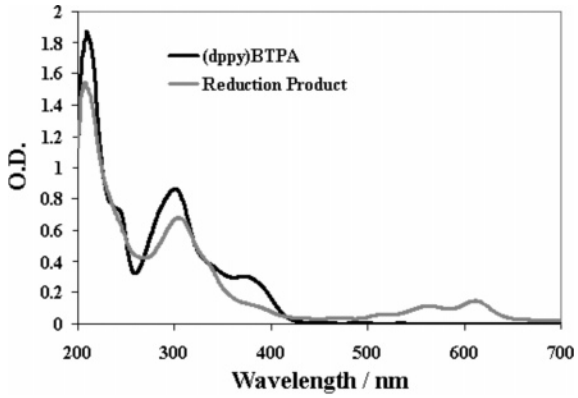

Figure 6. Absorbance spectra of (dppy)BTPA and its reduction product. Concentration ca. 25 μM.

Princeton Instruments Spec-10 CCD camera (Trenton, NJ) with an Acton SpectraPro-150 monochromator (Acton, MA). The integration time for all spectra was 5 min. The ECL spectra were calibrated using a Hg/Ar pen-ray lamp from Oriel (Stratford, CT). The ECL transients were obtained by connecting the Autotolab potentiostat to the output of a power meter for a photomultiplier tube (PMT, Hamamatsu R4220p, Japan) placed beneath the working electrode. The PMT was supplied with −750 V from a high-voltage power supply Series 225 (Bertan High Voltage Corp., Hucksville, NY).

The ECL efficiencies were estimated from current-normalized peak light intensities (averaged if the peaks varied in height) of the transients. The $Ru(bpy)_3^{2+}$ compound was used as the ECL standard with an excited-state generation efficiency of $\Phi_{ECL,Ru} \approx 0.65$ at 25 °C.[15] All ECL efficiency experiments were performed with a UME pulsed at 2.5 Hz between the oxidation and reduction potentials of the analyte, which yielded the optimum light intensity in the most resistive solution. The ECL efficiency will be described by two quantities: (1) ECL quantum yield ($\Phi_{ECL,QY}$), which refers to photons emitted per electron-transfer event; and (2) ECL quantum efficiency (Φ_{ECL}), which refers to excited states created per electron transfer. Both are defined by eqs 4 and 5, respectively,

$$\Phi_{ECL,QY} = \frac{I_X i_S}{I_S i_X} \Phi_{ECL,S} \Phi_{PL,S} \quad (4)$$

$$\Phi_{ECL} = \frac{I_X i_S \Phi_{PL,S}}{I_S i_X \Phi_{PL,X}} \Phi_{ECL,S} \quad (5)$$

where the subscript S refers to the ECL/PL standard, the subscript X refers to the analyte of interest, *I* refers to the light intensity measured by the power meter, and *i* refers to the observed faradaic current.

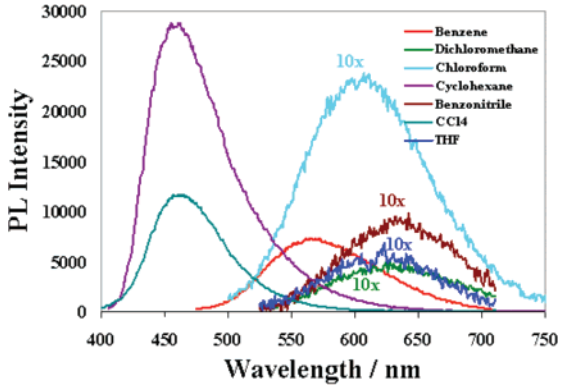

Figure 7. PL spectra of 10 μM (dppy)BTPA in various solvents. Spectra obtained in $CHCl_3$, benzonitrile, THF, and CH_2Cl_2 are magnified for clarity. Luminescence was not detected for (dppy)BTPA in acetonitrile under the concentration/slit width conditions used here.

Bulk electrolysis was performed in a three-compartment cell, with the compartments separated by fine porosity glass frits. The WE was a Pt wire grid placed in the first compartment. The RE, a Pt wire coated with polypyrrole,[16] was separated from the analyte solution by a glass tube sealed with a cracked glass junction. A magnetic stir bar was used to maintain uniform analyte concentration in the solution. The counter electrode was a Pt mesh placed in the third compartment. Each compartment contained MeCN with 0.1 M TBAP as the supporting electrolyte. The solution was electrolyzed for 15 min (until the current became constant) at $E_{p,red}$ − 100 mV.

Results and Discussion

Electrochemistry. Cyclic voltammetry was used to assess the energy of annihilation and to determine the stability of the (dppy)BTPA radical ions in solution. A cyclic voltammogram of (dppy)BTPA in MeCN is shown in Figure 2. The oxidation is a one-electron process occurring at $E^\circ_{ox} = 0.72$ V versus SCE that is reversible at scan rates (υ) as low as 50 mV/s, indicating stable radical cations. According to MO calculations, the HOMO, and hence the oxidation site, is mainly localized over the triphenylamine moiety.[3] The unusual stability of the radical cation may be attributed to the (dppy)B and butyl substituents at the para positions of each phenyl on the nitrogen, which prevent the dimerization reactions that typically accompany phenylamine oxidation.[17,18]

The reduction wave peak height is essentially the same as that of the oxidation; hence, it is also assigned as a one-electron process occurring at $E^\circ_{red} = -1.72$ V vs SCE. However, the reduction is less chemically reversible than the oxidation. In Figure 3, a plot of the anodic-to-cathodic peak current ratio (i_{pa}/i_{pc}) versus υ for various concentrations shows that, for lower concentrations, i_{pa}/i_{pc} approaches unity at lower scan rates than for high concentrations, indicating greater radical anion stability at lower concentrations. Concentration-dependent reversibility implies an EC process (a heterogeneous electron transfer followed by a homogeneous, chemical reaction) in which a dimerization reaction follows the electrochemical steps shown below (reactions 6 and 7).

$$(dppy)BTPA + e^- \rightarrow (dppy)BTPA^{\bullet -} \quad (6)$$

$$2(dppy)BTPA^{\bullet -} \leftrightarrows [(dppy)BTPA]_2^{2-} \quad (7)$$

TABLE 1: Absorbance and Photoluminescence Data for (dppy)BTPA in Various Solvents, and the Properties of the Solvents Listed in Order of Decreasing Solvent Polarizability (Δf)

solvent	$\lambda_{max,abs}$/nm	$\lambda_{max,PL}$/nm	PL quant. eff.	dielectric constant	refractive index	polarizability	Stokes shift /10^3 cm^{-1}
acetonitrile[a]	374	654	0.000 86	36.64	1.3442	0.3049	11.7
DMSO[a]	376	650	0.0012	47.24	1.4793	0.2633	11.6
1:1[a]	376	642	0.0042	19.46	1.4227	0.2596	11.2
benzonitrile	377	634	0.051	25.9	1.5289	0.236	10.9
3:1[a]	377	628	0.020	10.87	1.4619	0.2184	10.8
CH_2Cl_2	378	628	0.024	8.93	1.4242	0.217	10.7
THF	382	626	0.029	7.52	1.405	0.210	10.3
9:1[a]	379	611	0.068	5.718	1.4854	0.1565	10.2
$CHCl_3$	380	606	0.13	4.8069	1.4459	0.148 18	10.0
19:1[a]	381	599	0.12	4.000	1.4932	0.1081	9.7
CCl_4[b]	363	461	0.66	2.2379	1.4601	0.011 034	6.1
benzene[a]	382	564	0.40	2.2825	1.5011	0.002 8580	8.8
cyclohexane[b]	387	458	1.0[c]	2.0243	1.4235	−0.000 240	4.3

[a] The Φ_{PL} of these solvents was determined with respect to $Ru(bpy)_6(PF_6)_2$ in acetonitrile. All other Φ_{PL} were determined later, using (dppy)BTPA in benzene as the standard. [b] These solvents deviate from the Stokes shift-polarizability trend. [c] Rounded down from a measured value of 1.6. An impossibly measured Φ_{PL} is attributed to large error in successive normalizations.

TABLE 2: ECL Data for 1 mM (dppy)BTPA in Various Ratios of PhH/MeCN[a]

	$\lambda_{max,PL}$ /nm	$\lambda_{max,ECL}$/nm	E_s/eV	annihilation energy/eV	PL quant. efficiency	ECL exc. state eff.	ECL quant. yield
0:1	654	690	2.59	2.34	0.000 86	0.075	2.8×10^{-5}
1:1	638	670	2.61	2.42	0.0042	0.23	2.7×10^{-4}
3:1	634	657	2.62	2.50	0.020	0.15	6.4×10^{-4}
9:1	616	646	2.64	2.49	0.068	0.12	0.0015
19:1	604	637	2.65	2.54	0.12	0.078	0.0015

[a] PL data was obtained in solutions with 0.1 M TBAP.

CV simulations (Figures S1−S4, Supporting Information) using $K_{eq} = 10^5$ M^{-1} and $k_7 = 1.8 \times 10^4$ M^{-1} s^{-1} for the dimerization reaction (7) are in good agreement with the experimental data for $\upsilon = 0.05-10$ V/s over the concentration range 0.33−2.5 mM.

After scan reversal of the reduction wave at scan rates where the $A^{\bullet-}$ oxidation wave is small, a second oxidation wave appears with a peak potential of −0.59 V versus SCE (Figure 4). The dimer created in reaction 7 may undergo another following reaction, possibly with an impurity X (where X may be a proton or water) that results in a species of lower oxidation potential.

Additional information is obtained from reductive bulk electrolysis. After electrolysis, the light yellow solution of (dppy)BTPA converts to dark blue over the course of several hours. Seconds after exposure to air, the blue solution reverts to the yellow color of (dppy)BTPA. A mass spectrum of the electrolyzed compound after exposure to air shows a parent peak at the molecular weight of (dppy)BTPA, indicating reversal of the reduction and any following reactions. The difficulty of performing mass spectroscopy and nuclear magnetic resonance analysis while maintaining an inert atmosphere prevented us from analyzing the electrolysis product directly. Because oxidation in air yields the starting material, the −0.59 V oxidation peak may also be a conversion of the product back to the starting material. This data can be described by adding the following reactions to the dimerization (reactions 8−13).

$$[(dppy)BTPA]_2^{2-} \leftrightarrows P \quad (8)$$

$$[(dppy)BTPA]_2^{2-} + X \leftrightarrows [(dppy)BTPA]_2X^{2-} \quad (9)$$

$$[(dppy)BTPA]_2X^{2-} \rightarrow [(dppy)BTPA]_2X^{-} + e^{-} \quad (10)$$

$$[(dppy)BTPA]_2X^{-} \leftrightarrows [(dppy)BTPA]X^{-} + (dppy)BTPA \quad (11)$$

$$[(dppy)BTPA]X^{-} \rightarrow [(dppy)BTPA]X + e^{-} \quad (12)$$

$$[(dppy)BTPA]X \leftrightarrows (dppy)BTPA + X \quad (13)$$

The simulated and experimental data are compared in Figure S5 (Supporting Information). In the above mechanism, P represents a product generated in competition with reaction 9. Although reaction 8 is not discussed in chemical terms, its inclusion is necessary to accurately simulate the cyclic voltammogram at low υ values. However, the same simulation results can be created if P is a product of $[(dppy)BTPA]_2X^{2-}$ decomposition. The simulated impurity (X) was assigned a concentration of 3 μM. Because X has not been identified, the actual reaction may not be as described in reaction 9, but the close fit of the data suggests that the overall mechanism is correct. Product formation for reactions 8, 9, and 11 was treated as highly favorable and was assigned a K_{eq} value of 10^5, regardless of their units. The K_{eq} for reaction 13 was calculated from the other values and was found to be 9×10^{16} M. The rate constants assigned to these reactions are $k_8 = 0.045$ s^{-1}, $k_9 = 10^8$ M^{-1} s^{-1}, $k_{11} = k_{13} = 10^5$ s^{-1}. Rate constants k_9 and k_{11} were chosen arbitrarily, and only k_8 and k_9 were adjusted to fit the data. The first oxidation potential, $E^\circ_{10} = -0.55$ V vs SCE, was adjusted to fit the data, whereas $E^\circ_{12} = -1$ V was arbitrarily assigned to produce an ECE reaction (an EC process followed by additional heterogenous electron transfer at lower potential than the first). A two-electron oxidation creates peaks that are too narrow to fit the data, and a one-electron process does not generate sufficient current, even at high concentrations of X.

Spectroscopy. In pure MeCN, the absorbance spectrum of (dppy)BTPA, consists of a broad peak at 301 nm and a shoulder at 374 nm ($\epsilon = 1.1 \times 10^4$ M^{-1} cm^{-1}), which are attributed to absorption of the LUMO+4 and LUMO levels, respectively.[19] The absorbance spectra displayed little dependence of peak location on solvent polarizability, as shown in Figure 5. The long wavelength absorbance peak varied from 374 nm in pure MeCN to 382 nm in pure benzene. Absorbance of (dppy)BTPA in CCl_4 is unique because the LUMO and LUMO+4 peaks are the same height.

The absorbance spectrum of the electrolysis reduction product, shown in Figure 6, features a peak at 301 nm, similar to that of (dppy)BTPA, and additional peaks at 525, 569, and 612 nm. Excitation at those wavelengths yields no detectable luminescence. After exposure to air, the long-wavelength absorbance peaks disappear, and the 374 nm shoulder seen in (dppy)BTPA returns, indicating that the compound has reverted to its pre-electrolysis state.

The (dppy)BTPA fluorescence exhibits a strong bathochromic shift and a decrease in intensity as the solvent polarizability increases, as shown in Figure 7. In most solvents, the Stokes' shift of (dppy)BTPA can be described using the Lippert equation, which models the solvent relaxation of a molecule in an electronic excited-state by the solvent polarizability.[11] The polarizability (Δf) is a function of the dielectric constant (ϵ) and refractive index(n). Solvent orientation has a greater effect on excited-state energy for molecules with a strong dipole moment in the excited state, so CT emitters such as (dppy)-BTPA are expected to have large Stokes' shifts, as shown by the Lippert equation (eq 14),

$$\bar{\nu}_a - \bar{\nu}_f \cong \frac{2}{hc}\frac{(\mu^* - \mu)^2}{a^3}\Delta f + \text{const.} \qquad (14)$$

with the polarizability parameter given by eq 15.

$$\Delta f = \frac{\epsilon - 1}{\epsilon + 1} - \frac{n^2 - 1}{2n^2 + 1} \qquad (15)$$

The terms $\bar{\nu}_a$ and $\bar{\nu}_f$ are the absorbance and fluorescence wavenumbers, respectively, h is Plank's constant, c is the speed of light, a is the radius of the solvent cavity, and μ and μ^* are the ground and excited-state dipole moments, respectively. The data are given in Table 1. For pure solvents, literature values of ϵ and n were used;[20] for mixed solvents, they were calculated using linear combinations of n and ϵ based on the volume fraction of each solvent. A linear fit to the data was obtained in all solvents except CCl_4 and cyclohexane, which deviate significantly from the other solvents (Figure 8). The deviation could be because of scattering or the inability of the Lippert equation to account for specific interactions between the chromophore and the solvent. Because the electrolyte is insoluble in CCl_4 and cyclohexane, comparison between PL data and ECL data requires best-fit lines that exclude the two outlying points. However, if the deviation is merely data scattering, the two points should be included; therefore, the data has been plotted both ways. The cavity radius is estimated from X-ray data for (dppy)BTPA[3] to be 6 Å, which yields $\mu^* - \mu = 13$ D if CCl_4 and cyclohexane are excluded from the fit and 18 D if they are included. Both values are within the 9−44 D range of $\mu^* - \mu$ reported for other chromophores.[11]

The significant quenching that accompanies the bathochromic shift in the spectra is not understood, and it may consist of several factors. The primary contributor appears to be the energy gap law, which states that the nonradiative decay rate increases as the HOMO−LUMO energy gap decreases.[21] Plotting the fluorescence intensity against either solvent polarizability or viscosity did not yield a linear correlation. The apparent randomness of fluorescence intensity as a function of solvent viscosity rules out a twisted intramolecular charge transfer state as a quencher.[22] Furthermore, a solution of (dppy)BTPA in 60%/40% methanol/glycerol exhibited only 2× enhancement over (dppy)BTPA in pure methanol, whereas the lower viscosity 1:1 PhH/MeCN solutions led to a 5× enhancement in (dppy)BTPA emission over that of pure MeCN (Figure S6, Supporting Information). On the other hand, the addition of glycerol increases the polarizability of the glycerol−methanol solutions (Δf of glycerol = 0.74; Δf of methanol = 0.31), so the small enhancement contradicts the luminescence trend with respect to solvent polarizability, suggesting that viscosity does have a small effect. Adventitious water and oxygen are not significant quenchers, because MeCN solutions prepared in atmosphere are as luminescent as those prepared in the dry box. Strong PL quenching and a small bathochromic shift are also observed when the electrolyte TBAP is added to the solution (Figure S7, Supporting Information). Both effects are attributed to both the increased solvent dielectric and the specific interaction of the salt with the chromophore in a CT state.[23]

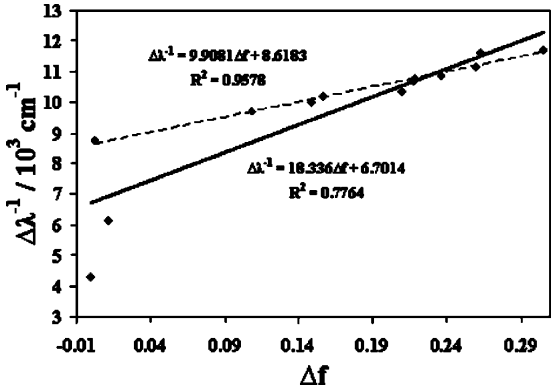

Figure 8. Lippert plot for (dppy)BTPA in various solvents without TBAP. The solid line fits all data points ($\mu^* - \mu = 18$ D), and the dotted line fits all the data except CCl_4 and cyclohexane ($\mu^* - \mu = 13$ D).

ECL. The electrogenerated chemiluminescence of (dppy)-BTPA was examined in solvents composed of various ratios of PhH to MeCN to examine the solvatochromism of the ECL. Table 2 summarizes the λ_{max}, quantum efficiency, and ECL data in the presence of 0.1 M TBAP. Intensity-normalized spectra are shown in Figure 9. The E_s was estimated as $hc(\bar{\nu}_a + \bar{\nu}_f)/2$.[24] According to these estimates, the annihilation energy is not sufficient to directly populate the excited singlet state, so the ECL must occur via the T-route. The $\Phi_{ECL,QY}$ increases as solvent polarizability decreases, following the trend observed for Φ_{PL}. However, Φ_{ECL} decreases when the PhH/MeCN ratio is greater than 1:1, although this may be because of the greater RC time constant and iR drop of low dielectric solvents.

The ECL spectra exhibit the same solvatochromic shift as the PL spectra. The ∼30 nm offset between the PL and ECL λ_{max} (Figure 10 and spectra in Figure S8, Supporting Information) is attributed to an instrumental artifact, because $\lambda_{max,PL} = \lambda_{max,ECL}$ when the CCD camera was used as a detector for photoluminescence of (dppy)BTPA in 19:1 PhH/MeCN excited by a Hg/Ar lamp (Figure S9, Supporting Information). Because absorbance is not relevant to ECL, $\bar{\nu}_f$, rather than the Stokes' shifts, is plotted against Δf. Because $\bar{\nu}_a$ is fairly constant, this

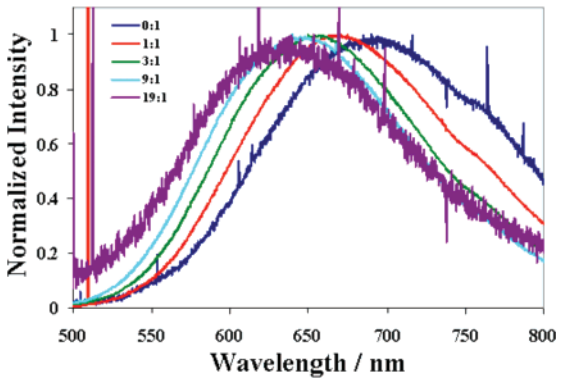

Figure 9. Normalized ECL spectra of (dppy)BTPA in various ratios of PhH/MeCN.

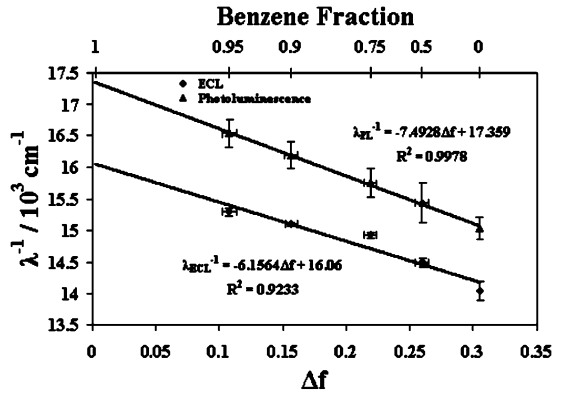

Figure 10. Lippert plots for PL and ECL of (dppy)BTPA in various mixtures of benzene/acetonitrile with 0.1 M TBAP. The *y*-axis is the fluorescence wavenumber rather than the Stokes shift, because ECL has no absorbance. $\mu^* - \mu = 11$ D for PL and 10 D for ECL.

should have little effect on the slope. The values for $\mu^* - \mu$ are 11 D for the PL plot and 10 D for the ECL plot.

The ECL spectra show solvent-independent emissions beyond 725 nm that are not present in the PL spectra. Long-wavelength features specific to ECL usually originate from annihilation phenomena, such as exciplex formation brought about by the proximity of the radical ions, reaction of a radical ion with an impurity, or emission from an intermediate or side product. However, this emission was also observable at the same relative intensity when BPO was used as a coreactant with (dppy)BTPA to generate emission without annihilation. On the other hand, annihilation can still occur if the coreactant oxidizes the analyte, so this is not conclusive.[25]

The strong dipole moment in the excited-state and the proximity of two radical ions during annihilation are conducive to exciplex formation. Emission from a side product cannot be ruled out, however, because $[(dppy)BTPA]_2X^{2-}$ may produce detectable emission during ECL, even though it was too dilute to detect in the PL spectrum of the electrolyzed solution.

Conclusions

The strong CT character of (dppy)BTPA leads to a bathochromic shift in PL and ECL, as well as dramatic excited-state quenching as the solvent polarizability is increased. While the radical cation of (dppy)BTPA is surprisingly stable, the radical anion dimerizes with $k_f = 1.8 \times 10^4\ M^{-1}\ s^{-1}$. The dimer can either react with impurities to form a species that is oxidizable back to (dppy)BTPA, or at a much slower rate, it can form another product that may be a polymer. The ECL spectrum closely resembles the fluorescence spectrum in each solvent, but it has the added feature of a shoulder at long wavelength that may result from an intermediate following radical anion decomposition.

Acknowledgment. We thank BioVeris Corp. and the National Science Foundation (CHE-0451494) for support of this research.

Supporting Information Available: Additional CVs (Figures S1−S5) and spectra (Figures S6−S8). This material is available free of charge via the Internet at http://pubs.acs.org.

References and Notes

(1) Li, Y.; Bu, W.; Guo, J.; Wang, Y. *Chem. Commun.* **2000**, 1551.
(2) Yang, G.; Liao, Y.; Su, Z.; Zhang, H.; Wang, Y. *J. Phys. Chem. A* **2006**, *110*, 8758.
(3) Zhang, H.; Huo, C.; Zhang, J.; Zhang P.; Tian, W.; Wang, Y. *Chem. Commun.* **2006**, 281.
(4) For reviews on ECL, see: (a) *Electrogenerated Chemiluminescence*; Bard, A., Ed.; Marcel Dekker, Inc.: New York, **2004**. (b) Richter, M. M. *Chem. Rev.* **2004**, *104*, 3003−3036. (c) Knight, A. W.; Greenway, G. M. *Analyst* **1994**, *119*, 879−890.(d) Faulkner, L. R.; Bard, A. J. *Electroanalytical Chemistry*; Marcel Dekker: New York, 1977; Vol. 10, p 1. (e) Bard, A. J.; Debad, J. D.; Leland, J. K.; Sigal, G. B.; Wilbur, J. L.; Wohlstadter, J. N. In *Encyclopedia of Analytical Chemistry: Applications, Theory and Instrumentation*; Meyers, R. A., Ed.; John Wiley & Sons: New York, 2000; Vol. 11, p 9842.
(5) Akins, D. L.; Birke, R. L. *Chem. Phys. Lett.* **1974**, *29*, 428.
(6) Chandross, E.; Sonntag, F. *J. Am. Chem. Soc.* **1966**, *88*, 1089.
(7) Choi, J.-P.; Wong, K.-T.; Chen, Y.-M.; Yu, J.-K.; Chou, P.-T.; Bard, A. *J. Phys. Chem. B* **2003**, *107*, 14407.
(8) (a) Kapturkiewicz, A.; Grabowski, Z.; Jasny, J. *J. Electroanal. Chem.* **1990**, *279*, 55. (b) Kapturkiewicz, A. *J. Electroanal. Chem.* **1991**, *302*, 131. (c) Kapturkiewicz, A. *Chem. Phys.* **1992**, *166*, 259. (d) Kapturkiewicz, A.; Herbich, J.; Nowacki, J. *Chem. Phys. Lett.* **1997**, *275*, 355.
(9) Kapturkiewicz, A. *Z. Phys. Chem. NF*. **1991**, *170*, 87.
(10) Kapturkiewicz, A. *J. Electroanal. Chem.* **1990**, *290*, 135.
(11) Lackowicz, J. R. *Principles of Fluorescence Spectroscopy*; Plenum Press: New York, 1983; pp 189−208.
(12) Sahami, S.; Weaver, M. *J. Electroanal. Chem.* **1981**, *122*, 155.
(13) (a) Rudolph, M. *J. Electroanal. Chem.* **2003**, *543*, 23. (b) Ruldolph, M. *J. Electroanal. Chem.* **2004**, *571*, 289. (c) Rudolph, M. *J. Electroanal. Chem.* **2003**, *558*, 171. (d) Rudolph, M. *J. Comp. Chem.* **2005**, *26*, 619. (e) Rudolph, M. *J. Comp. Chem.* **2005**, *26*, 633. (f) Rudolph, M. *J. Comp. Chem.* **2005**, *26*, 1193.
(14) Kadish, K.; Ding, J.; Malinski, T. *Anal. Chem.* **1984**, *56*, 1741.
(15) Wallace, W.; Bard, A. *J. Phys. Chem.* **1979**, *83*, 1350.
(16) Ghilane, J.; Hapiot, P.; Bard, A. *Anal. Chem*. **2006**, *78*, 6868.
(17) Eberson, L. In *Organic Electrochemistry*; Baizer, M., Ed.; Marcel Dekker: New York, 1973; pp 518−520.
(18) Seo, E.; Nelson, R.; Fritsch, J.; Marcoux, L.; Adams, R. J. *Am. Chem. Soc*. **1966**, *88*, 3498.
(19) Yang, G.; Liao, Y.; Su, S.; Zhang, H.; Wang, Y. *J. Phys. Chem. A* **2006**, *110*, 8758.
(20) *Handbook of Chemistry and Physics*, 87th ed., 2006−2007. http://www.hbcpnetbase.com/; accessed 10/23/06.
(21) (a) Caspar, J.; Kober, E.; Sullivan, B.; Meyer, T. *J. Am. Chem. Soc*. **1982**, *104*, 630. (b) Englman, R.; Jortner, J. *Molecular Physics* **1970**, *18*, 145.
(22) (a) Morimoto, A.; Biczók, L.; Yatsuhashi, T.; Shimada, T.; Baba, S.; Tachibana, H.; Tryk, D.; Inoue, H. *J. Phys. Chem. A* **2002**, *106*, 10089. (b) Willets, K.; Callis, P.; Moerner, W. *J. Phys. Chem. B* **2004**, *108*, 10465. (c) Anni, M.; Sala, F.; Raganato, M.; Fabiano, E.; Lattante, S.; Cingolani, R.; Gigli, G. *J. Phys. Chem. B* **2005**, *109*, 6004.
(23) (a) Chapman, C.; Maroncelli, M. *J. Phys. Chem.* **1991**, *95*, 9095. (b) Huppert, D.; Bart, E. *Chem. Phys. Lett*. **1992**, *195*, 37. (c) Lavalle, R.; Zimmt, M. *J. Phys. Chem*. **1994**, *98*, 4254.
(24) Marcus, R. A. *J. Phys. Chem*. **1989**, *93*, 3078.
(25) Fabrizio, E.; Prieto, I.; Bard, A. *J. Am. Chem. Soc*. **2000**, *122*, 4996.